Optical Spectroscopy: Probing Atomic Structure

Jason Gross*
Student at MIT
(Dated: December 2, 2011)

Using a mercury-calibrated monochrometer, we measured the spectra of three atoms: hydrogen, deuterium, and sodium. From the hydrogen spectrum, I verify the usefulness of the Bohr model of the atom, determine the accuracy of the Balmer/Bohr formula for wavelengths, and calculate the Rydberg constant to be $R_H = 0.001\,097\,044(8)\ \text{Å}^{-1}$ as compared with an accepted value from NIST of $0.001\,096\,775\,834\,065(38)\ \text{Å}^{-1}$. Measurement of the Balmer lines for deuterium permits calculation of the deuterium-to-hydrogen nuclear mass ratio; taking the electron mass to be $9.109\,382\,91(40)\cdot 10^{-31}$ kg (NIST), I find the mass of the ratio to be 2.043 29(62), as compared with an accepted value from NIST of 1.999 007 50(44), respectively. I note a splitting of the $n = 3 \longrightarrow n = 2$ peak in the hydrogen and deuterium spectra of (0.1389 ± 0.0071) Å and (0.1424 ± 0.0020) Å, respectively. The first-order relativistic and spin-coupling corrections to the Hamiltonian are invoked to explain this effect, yielding predicted separations of
FIX
.
From the sodium spectrum I construct an energy level diagram for sodium. The fine structure of the sodium spectrum is analyzed, and the Landé formula is verified.
FIX

I. THEORY

I.1. Spectroscopy

FIX

I.2. The Bohr Model

In 1888, Johannes Rydberg found that the spectral lines of hydrogen obey the formula

$$\frac{1}{\lambda} = R\left(\frac{1}{n_f^2} - \frac{1}{n_i^2}\right)$$

with n_f and n_i integers. Following Bohr and [1], if we treat the electron as a classical charged particle in a circular orbit around the center of mass of the atom, we find that the energy of an electron is

$$E = \frac{1}{2}m_e v^2 - \frac{e^2/4\pi\varepsilon_0}{r} = -\frac{e^2/4\pi\varepsilon_0}{2r}.$$

I.3. Spin-Orbit Coupling

I.4. Relativistic Correction

I.5. Emperical Formula for Alkali Metals

II. EXPERIMENTAL SETUP

The spectra were taken using a Czerny-Turner monochromator; our setup is shown in Figure 1. Light from the source is reflected onto a grating, which diffracts the light before it is measured by a photomultiplier tube (PMT). The angle of the grating, controlled by a computer, determines which wavelength of light lines up with the entrance of the PMT.

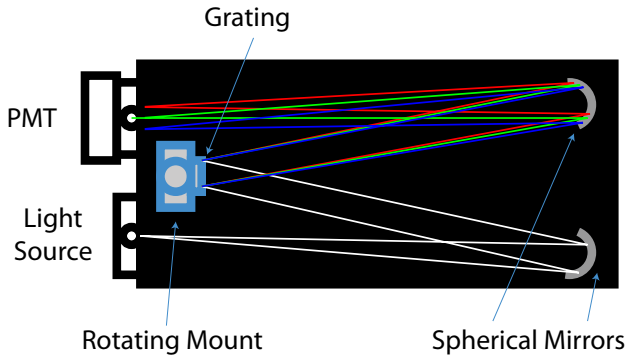

FIG. 1. Light from the source is collimated via a spherical mirror onto a flat grating on a rotating mount controlled via computer. The grating diffracts light on to a second spherical mirror, which focuses the light on to a photomultiplier tube (PMT). The PMT is connected to a computer for reading. The angle of the grating determines which wavelength of light experiences constructive interference at the angle required to arrive at the small slit leading to the PMT.

III. CALIBRATION

Although the angle of the grating in the monochromator is controlled by setting a wavelength, the machine's wavelength to angle converter was found to be inaccurate. We measured various peaks in the spectrum of mercury and calibrated the monochromator's reading against ac-

* jgross@mit.edu

cepted values for the peaks from [2].

From 46 distinct measurements, I extracted 111 peaks (not all distinct) in the mercury spectrum. Peaks consisting of only a few points were taken to be centered at their maxima, with an uncertainty of half the step size. All other peaks were, for simplicity, fit to Gaussians, using half the step-size as the uncertainty in λ and Poisson errors on photon count rates. Because many of the peaks did were not well-modeled by Gaussians (see Figure 2), I multiplied the uncertainty in the mean by χ_ν to obtain a slightly better estimate (see §6.4 in [3]).

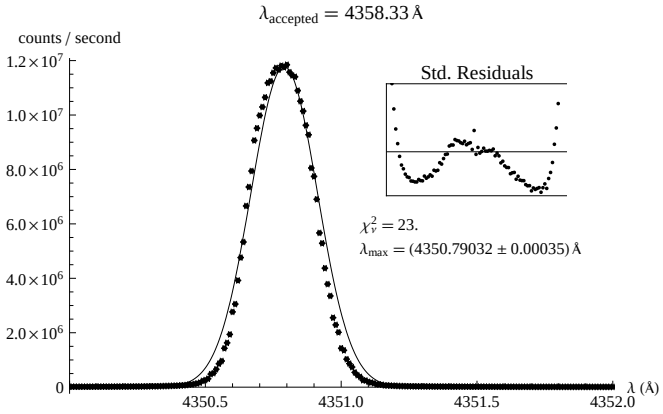

FIG. 2. Typical example of Gaussian fit to a mercury peak. The region in which the function was fit was chosen to be the set of points which, given the level of noise we were seeing, we'd expect to see less than once if we took this same spectrum 100 times. Note the smallness of the uncertainty and the asymmetry of the fit relative to the peak.

Nine particularly unambiguous peaks (judged by a combination of intensity and isolation from other peaks) were chosen as the basis of the calibration. The differences between accepted peak value and observed peak value were clearly non-linear ($\chi^2_\nu \approx 10^4$ and the residuals were systematic), and fit relatively well to a quadratic ($\chi^2_\nu \approx 300$, no obvious systematicity in the residuals).

Using this quadratic fit, I further refined the calibration by incorporating all peaks that were within 1–2 Åof the predicted wavelength of some peak in [2]. This resulted in a total of 45 observed peaks, each associated with one of 17 accepted peaks. Due to an oversight, we did not to ensure that the voltage setting on the light source was the same for all readings and neglected to record its values; the intensity of the peaks are not sufficiently reliable to allow for quantitative comparison with accepted intensities. The final fit is shown in Figure 3.

I believe that the errors on most of the peaks, even after refinement, are vastly underestimated. Multiplying the uncertainties on the individual peak means by χ_ν gives a better estimate of what the uncertainties would be, if the data were Gaussian; in a sense, it weights the data points by how close to Gaussian they are. If we assume that the offset $\delta\lambda$ is quadratic in $\lambda_{\text{measured}}$, then we may get a better estimate of the errors on the calibration

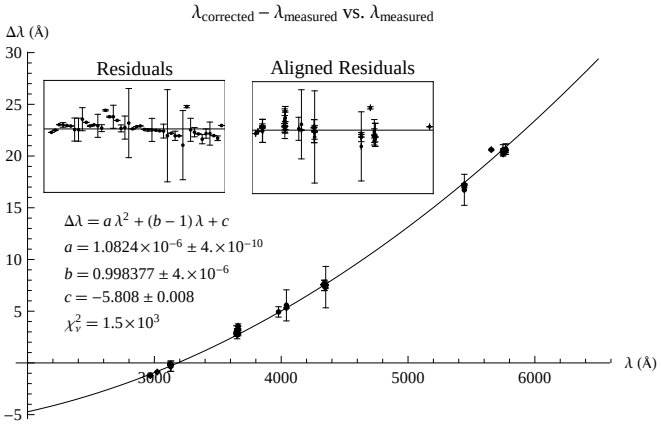

FIG. 3. Mercury calibration plot. The aligned residual plot is a plot of residual vs. λ; the residual plot is a plot of residual vs. point number. The vertical scale on the residual plots is from approximately -1.5Åto 1.5Å. Ticks are not shown to conserve space. The residuals plots include error bars which combine the fit parameter errors with the uncertainties in λ. Some of the errors are, unfortunately, double-counted; for simplicity, I treat λ, λ^2, a, b and c as independent variables.

fit parameters by multiplying by χ_ν. Doing so gives

$$\begin{aligned}\Delta\lambda &= a\lambda^2 + b\lambda + c\\ a &= (1.082 \pm 0.015)\cdot 10^{-6}\,\text{Å}^{-1}\\ b &= 0.998\,38 \pm 0.000\,14\\ c &= (5.81 \pm 0.32)\,\text{Å}\end{aligned}$$

where $\lambda \equiv \lambda_{\text{measured}}$ and $\Delta\lambda \equiv \lambda_{\text{accepted}} - \lambda_{\text{measured}}$.

IV. BOHR MODEL

IV.1. Hydrogen and Deuterium

The Bohr model predicts that the wavelengths of peaks for a hydrogenic atom of mass M obey the formula

$$\frac{1}{\lambda} = \frac{M}{m_e + M} R_\infty \left(\frac{1}{n_i^2} - \frac{1}{n_f^2}\right)$$

where m_e is the mass of the electron, R_∞ is a constant, and n_i and n_f are positive integers. We measured the peaks corresponding to the first seven Balmer lines ($n_f = 2$), (a typical uncalibrated fit is shown in Figure 4) obtaining calibrated wavelengths of

Deuterium Peak (Å)	Hydrogen Peak (Å)	Peak Separation (Å)
3834.43 ± 0.66	3835.62 ± 0.66	1.1900 ± 0.0050
3888.04 ± 0.66	3889.25 ± 0.66	1.2057 ± 0.0021
3969.08 ± 0.68	3970.40 ± 0.68	1.3195 ± 0.0020
4100.79 ± 0.70	4101.86 ± 0.70	1.0656 ± 0.0010
4339.20 ± 0.73	4340.54 ± 0.73	1.33265 ± 0.00070
4859.99 ± 0.82	4861.37 ± 0.82	1.38172 ± 0.00060
6561.3 ± 1.1	6563.0 ± 1.1	1.71204 ± 0.00064

and fit the data, as shown in Figure 5.

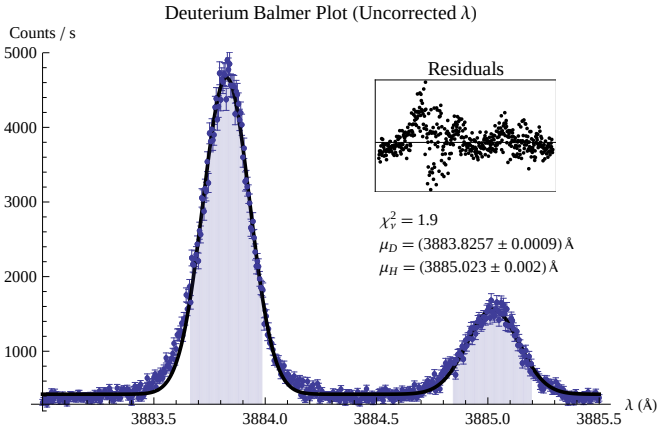

FIG. 4. Peak data for a typical peak from the deuterium spectrum. The source tube contained enough hydrogen to get hydrogen and deuterium peaks from the same measurement. The peaks were fit using only the data in the shaded region.

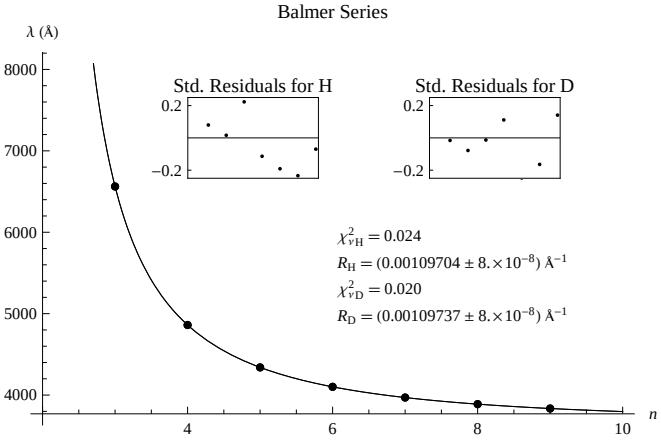

FIG. 5. Plot of λ vs. n for the Balmer lines for hydrogen and deuterium. Residual plots are of standardized residuals.

Solving the Balmer/Bohr formula for $\lambda_D - \lambda_H$, the isotope shift due to the difference in mass between deuterium and hydrogen, gives

$$\lambda_D - \lambda_H = \lambda_H \left(\frac{\frac{m_e}{M_d} + 1}{\frac{m_e}{M_p} + 1} - 1 \right)$$

where M_d is the nuclear mass of the deuteron and M_p is the nuclear mass of hydrogen, which is the mass of a proton. Taking the electron to proton mass ratio to be $5.446\,170\,22(24) \cdot 10^{-7}$ ([4, 5]), fitting the peak differences to this formula (Figure 7) gives $m_d/m_p = 2.043\,29(62)$, as compared with an accepted value of $1.999\,007\,50(44)$ ([6]).

In the highest energy hydrogen/deuterium peak, there is obvious, if slight, peak splitting, as shown in **??**

$$\lambda_H - \lambda_D = \lambda_D \left(\frac{\frac{m_e}{M_p} + 1}{\frac{m_e}{M_d} + 1} - 1 \right)$$

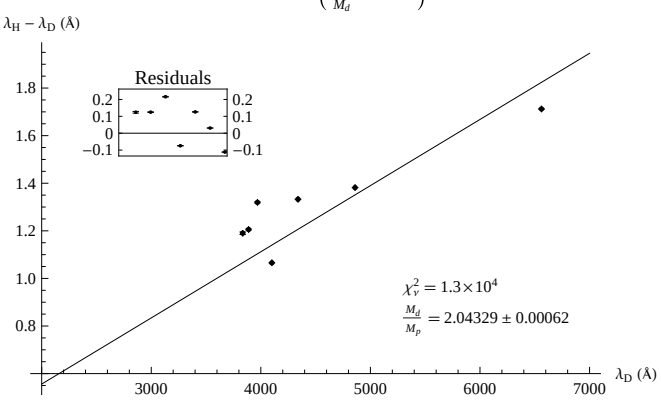

FIG. 6. Plot of peak differences vs. peak wavelength.

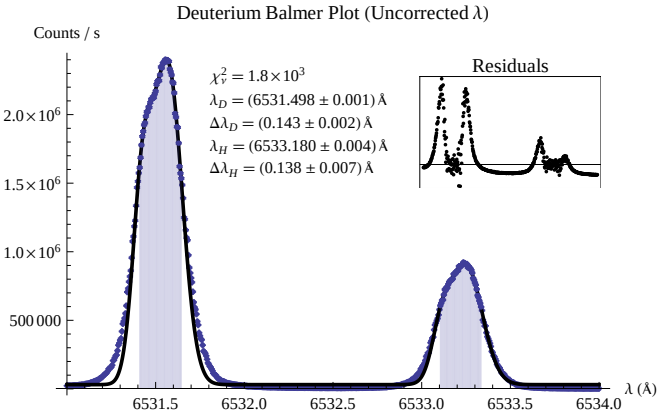

FIG. 7. Plot of fine structure of the highest energy hydrogen/deuterium peak that we measured. Peaks were fit to the sum of two Gaussians, using the data in the shaded region. χ^2_ν is taken over the entire spectrum. λ is the average of the two means, $\Delta\lambda$ is the difference between the means.

V. FINE STRUCTURE: SODIUM

We found the following sodium peaks:

(4735.965 ± 0.012) Å
(4742.158 ± 0.012) Å
(5662.3694 ± 0.0050) Å
(5663.0451 ± 0.0050) Å
(5668.6211 ± 0.0050) Å
(5669.9698 ± 0.0036) Å
(5868.2331 ± 0.0050) Å
(5874.3618 ± 0.0050) Å
(6130.60 ± 0.15) Å
(6136.200 ± 0.075) Å
(4485.60 ± 0.10) Å
(4489.20 ± 0.10) Å
(5670.3223 ± 0.0090) Å

VI. CONCLUSIONS

[1] C. J. Foot, *Atomic Physics*, Vol. 7 (Oxford University Press, USA, 2005).
[2] J. E. Sansonetti and W. C. Martin, Journal of Physical and Chemical Reference Data **34**, 1559 (2005).
[3] P. Bevington and D. Robinson, *Data Reduction and Error Analysis for the Physical Sciences* (McGraw-Hill, 2003).
[4] "CODATA value: electron mass," (2010).
[5] "CODATA value: proton mass," (2010).
[6] "CODATA value: deuteron mass," (2010).

ACKNOWLEDGMENTS

The author gratefully acknowledges his lab partner Thomas Vandermeulen for help collecting the data, and the J-Lab staff for their help in experimentation.